

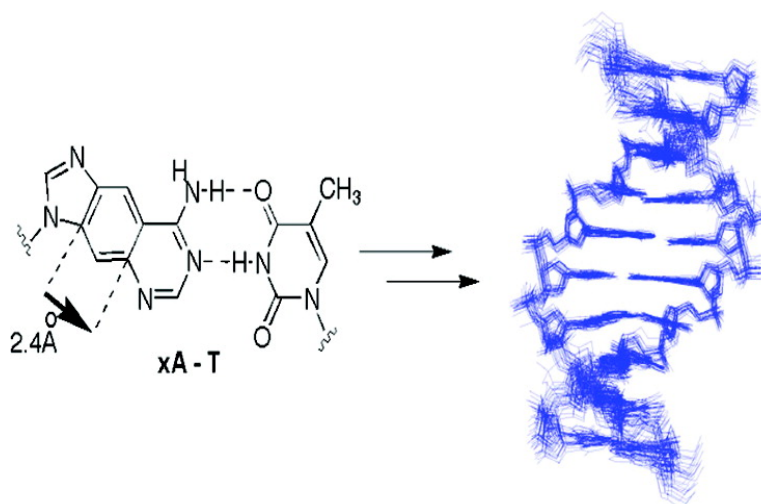
Article

**Solution Structure of xDNA: A Paired Genetic Helix with Increased Diameter**

Haibo Liu, Stephen R. Lynch, and Eric T. Kool

*J. Am. Chem. Soc.*, **2004**, 126 (22), 6900-6905 • DOI: 10.1021/ja0497835 • Publication Date (Web): 08 May 2004

Downloaded from <http://pubs.acs.org> on March 31, 2009



**More About This Article**

Additional resources and features associated with this article are available within the HTML version:

- Supporting Information
- Links to the 10 articles that cite this article, as of the time of this article download
- Access to high resolution figures
- Links to articles and content related to this article
- Copyright permission to reproduce figures and/or text from this article

[View the Full Text HTML](#)



**ACS Publications**  
 High quality. High impact.

## Solution Structure of xDNA: A Paired Genetic Helix with Increased Diameter

Haibo Liu, Stephen R. Lynch, and Eric T. Kool\*

Contribution from the Department of Chemistry, Stanford University,  
Stanford, California 94305-5080

Received January 13, 2004; E-mail: kool@stanford.edu

**Abstract:** We describe the structure in aqueous solution of an extended-size DNA-like duplex with base pairs that are  $\sim 2.4$  Å longer than those of DNA. Deoxy-*lin*-benzoadenosine (dxA) was employed as a dA analogue to form hydrogen-bonded base pairs with dT. The 10mer self-complementary extended oligodeoxynucleotide 5'-d(xATxAxATxATTxAT) forms a much more thermodynamically stable duplex than the corresponding DNA sequence, 5'-d(ATAATATTAT). NMR studies show that this extended DNA (xDNA) retains many features of natural B-form DNA, but with a few structural alterations due to its increased helical diameter. The results give insight into the structural plasticity of the natural DNA backbone and lend insight into the evolutionary origins of the natural base pairs. Finally, this structural study confirms the hypothesis that extended nucleobase analogues can form stable DNA-like structures, suggesting that alternative genetic systems might be viable for storage and transfer of genetic information.

### Introduction

Chemists have recently worked on approaches to replacing individual base pairs within the overall geometry of natural DNA.<sup>1–5</sup> Adopting a different strategy, we envisioned that an alternative way to alter base pairs would be to increase their size but retain the natural phosphodiester backbone.<sup>6</sup> This of course raises the questions whether such added size can be tolerated structurally and what adjustments in backbone and helical structure would be needed to accommodate this geometric change.

The study of altered DNA structures and stabilities also can give insight into the plasticity of natural DNA itself. What are the energetic penalties for DNA distortion? How does distortion of DNA base-pair structure affect backbone stability and conformation? How does it affect the active sites (and activities) of DNA-processing enzymes?

Beyond the implications of these questions in evolution and biology in general, one may also ask the structural questions of the double helix for applications in molecular design. DNA is becoming increasingly adopted as a scaffold for self-assembling

nanostructures.<sup>7</sup> Could other structures be used besides that of natural DNA?

As an initial foray into answering these questions, we examined the structure of an extended DNA (xDNA) double helix. We recently described the molecular design of xDNA, in which DNA bases are extended in size by addition of a benzene ring.<sup>6</sup> Early studies were carried out to evaluate pairing abilities of extended adenine and thymine bases. Remarkably, such extended bases were found to form surprisingly stable helices. However, structural studies are needed to better understand the origins of such stability and to answer the above questions about the basic properties of DNA. Thus, we undertook a structural study in solution by 2D NMR.

For this first study, we chose the simplest case, involving only one expanded base, Leonard's *lin*-benzoadenine.<sup>8</sup> In combination with T, we have shown that it forms a two-base genetic system with the pairs T-xA and xA-T.<sup>6</sup> Here we show that the DNA backbone is surprisingly forgiving to such a considerable stretch to the base-pair structure and that this xDNA duplex has only small conformational differences from the normal conformational preferences of natural B-form DNA. The results underscore the importance of homogeneity in backbone and base-pair structure for stability of the double helix.

### Experimental Section

**Sample Preparation.** The xA phosphoramidite was synthesized<sup>6b</sup> and incorporated into a self-complementary DNA-like 10mer, 5'-d(xATxAxATxATTxAT), using an Applied Biosystems 394 DNA/RNA synthesizer. After the oligonucleotide was synthesized without trityl protection on 5'-OH, it was purified by preparative denaturing poly-

- (1) Piccirilli, J. A.; Krauch, T.; Moroney, S. E.; Benner, S. A. *Nature* **1990**, *343*, 33–37.
- (2) Rappaport, H. P. *Nucleic Acids Res.* **1988**, *16*, 7253–7267.
- (3) (a) Schweitzer, B. A.; Kool, E. T. *J. Am. Chem. Soc.* **1995**, *117*, 1863–1872. (b) Matray, T. J.; Kool, E. T. *J. Am. Chem. Soc.* **1998**, *120*, 6191–6192. (c) Matray, T. J.; Kool, E. T. *Nature* **1999**, *399*, 704–708.
- (4) (a) McMinn, D. L.; Ogawa, A. K.; Wu, Y. Q.; Liu, J. Q.; Schultz, P. G.; Romesberg, F. E. *J. Am. Chem. Soc.* **1999**, *121*, 11585–11586. (b) Tae, E. J. L.; Wu, Y. Q.; Xia, G.; Schultz, P. G.; Romesberg, F. E. *J. Am. Chem. Soc.* **2001**, *123*, 7439–7440. (c) Mitsui, T.; Kitamura, A.; Kimoto, M.; To, T.; Sato, A.; Hirao, I.; Yokoyama, S. *J. Am. Chem. Soc.* **2003**, *125*, 5298–5307.
- (5) (a) Meggers, E.; Holland, P. L.; Tolman, W. B.; Romesberg, F. E.; Schultz, P. G. *J. Am. Chem. Soc.* **2000**, *122*, 10714–10715. (b) Tanaka, K.; Tengeiji, A.; Kato, T.; Toyama, N.; Shionoya, M. *Science* **2003**, *299*, 1212–1213.
- (6) (a) Liu, H.; Gao, J.; Lynch, S. R.; Saito, Y. D.; Maynard, L.; Kool, E. T. *Science* **2003**, *302*, 868–871. (b) Liu, H.; Gao, J.; Saito, Y. D.; Maynard, L.; Kool, E. T. *J. Am. Chem. Soc.* **2004**, *126*, 1102–1109.

(7) Seeman, N. C. *Nature* **2003**, *421*, 427–431.

(8) Leonard, N. J.; Sprecker, M. A.; Morrice, A. G. *J. Am. Chem. Soc.* **1976**, *98*, 3987–3994.

acrylamide gel electrophoresis (PAGE). The purity was found to be greater than 95% as checked by analytical PAGE. The oligonucleotide was desalted by extensive dialysis washing, followed by further centrifugal filtration with Microcon (Millipore Co., Bedford, CA), YM3000 (NMWC = 3000). The sample was dissolved in buffer (10 mM sodium phosphate, pH 7.0) at a final concentration of 1.3 mM.

**Thermal Denaturation.** Total oligonucleotide concentration was 2.0–12.0  $\mu$ M in various experiments. The buffer contained NaCl (100 mM), MgCl<sub>2</sub> (10 mM), and Na-PIPES (10 mM) at pH 7.0. Samples were heated at 95 °C for 10 min, then allowed to cool to room temperature slowly for at least 2 h, followed by cooling at 0–5 °C for at least 4 h. Melting studies were carried out in Teflon-stopped 1 cm path length quartz cells (under nitrogen atmosphere when temperature is below 20 °C) on a Varian Cary One UV–visible spectrophotometer equipped with a thermoprogrammer. Absorbance was monitored while temperature was increased at a rate of 0.5 °C/min. Experiments were monitored at 260 or 325 nm for normal and extended sequences, respectively. The complexes displayed apparent two-state transitions, with all-or-none melting curves from bound duplex to free single strands. Computer fitting, using MeltWin 3.0b, of the melting data provided both melting temperatures ( $T_m$ ) and free energy values for the complexes. Free energies were also calculated from van't Hoff plots by plotting  $1/T_m$  vs  $\ln(C/4)$ ; in both cases close agreement was observed, indicating that the two-state approximation is not unreasonable for these specific sequences.

**NMR Spectroscopy.** NMR experiments were acquired on either a Varian Inova 600 MHz NMR instrument or Varian Inova 500 MHz NMR instrument equipped triple resonance and z-gradient or triple axis gradient capabilities. NMR spectra were acquired at 35 °C in 99.996% D<sub>2</sub>O buffer or at 15, 25, and 35 °C in 90% H<sub>2</sub>O/10% D<sub>2</sub>O buffer. Resonances were assigned with standard methods using a combination of <sup>31</sup>P-decoupled DQF-COSY, TOCSY, <sup>13</sup>C/<sup>1</sup>H HSQC, <sup>31</sup>P/<sup>1</sup>H heteronuclear COSY, NOESY, WET-NOESY, and SS-NOESY experiments. TOCSY experiments were acquired with mixing times of 20 and 80 ms. NOESY experiments in D<sub>2</sub>O were acquired with mixing times of 50, 100, 150, and 300 ms. SS-NOESY and WET-NOESY experiments were acquired in 90% H<sub>2</sub>O with mixing times of 75 and 150 ms.

The protons on the deoxyribose residues were distinguished by type with <sup>13</sup>C/<sup>1</sup>H HSQC acquired in natural abundance and separated into nucleotide spin systems with TOCSY and DQF-COSY. The deoxyribose protons were correlated to the base with strong intranucleotide NOEs between H2' and H6 for thymidine, and H1' and H4 and the H2' and H2 for xA. The imino protons of thymidine could be assigned based upon imino–imino NOEs between sequential base pairs and strong NOEs to the H6 proton of the xA. Proton assignment and NOE signal integration were carried out using SPARKY 3.<sup>9</sup>

**Structure Calculation.** Structures of the 10 base-pair self-complementary sequence were calculated on an SGI Octane workstation with restrained molecular dynamics followed by energy minimization with the program CNS.<sup>10</sup> Thirty random starting structures were created by giving different initial velocities to an elongated single-stranded DNA. These structures were subjected to a simulated annealing protocol with restrained torsion angle dynamics utilizing a force field of bond lengths, bond angles, improper angles, repulsive van der Waals potentials, and experimental distance and torsion angle constraints. Of 30 structures, 24 converged to low energy and were subjected to a second stage of refinement; this was followed by a final energy minimization that included all of the above constraints in addition to attractive Lennard-Jones potentials. Electrostatic potentials were not included at any stage of the calculation. The final structures were

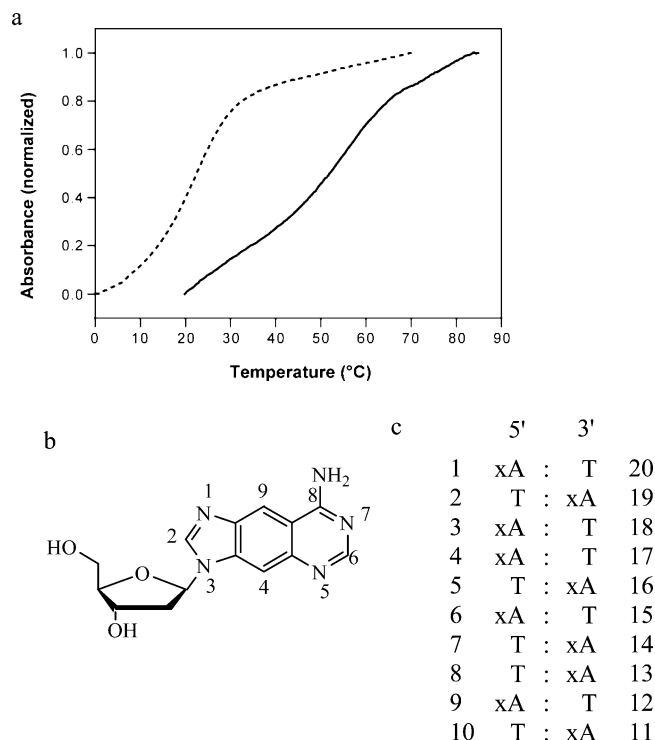


**Figure 1.** (a) Thermal denaturation curves of xDNA (monitored at 325 nm, solid line) and of DNA of analogous sequence (monitored at 260 nm, dotted line). Sequence of the xDNA is xATxAxATxATTxAT, and that of DNA is ATAATATTAT. These are self-complementary sequences shown to form duplexes. (b) Numbering of atoms in the xA deoxynucleoside. (c) Numbering of residues in xDNA duplex.

superimposed and displayed with either the program MOLMOL<sup>11</sup> or Insight II (Accelrys, San Diego, CA).

Distance restraints for nonexchangeable protons were assigned based upon analysis of cross-peak intensity in D<sub>2</sub>O NOESY experiments with mixing times of 50, 100, 150, and 300 ms and a WET-NOESY experiment in H<sub>2</sub>O with 150 ms mixing time. NOEs were assigned as strong (1.8–3.0 Å), medium (2.5–4.0 Å), and weak (3.0–6.0 Å). NOEs to thymidine imino protons were assigned in SS-NOESY experiments at 75 and 150 ms. Hydrogen bonds for the Watson–Crick-like base pairs were assigned based upon strong NOEs observed between the thymine imino-H and xA H6 as well as the downfield chemical shift of the thymidine imino resonance.

Dihedral constraints were assigned based on analysis of DQF-COSY and <sup>31</sup>P/<sup>1</sup>H heteronuclear COSY. The sugar pucker was constrained based upon comparison of <sup>3</sup>J<sub>H1'H2'</sub>, <sup>3</sup>J<sub>H1'H2''</sub>, and <sup>3</sup>J<sub>H3'H4'</sub> values. All nucleotides were determined to be C2'-endo. The backbone torsion angle  $\beta$  was estimated based upon measurement of <sup>3</sup>J<sub>H5'P</sub>, <sup>3</sup>J<sub>H5''P</sub>, and <sup>4</sup>J<sub>H4'P</sub>. The backbone torsion angle  $\gamma$  was estimated based upon measurement of <sup>3</sup>J<sub>H4'H5'</sub>, <sup>3</sup>J<sub>H4'H5''</sub>, and <sup>4</sup>J<sub>H4'P</sub>. Each was assigned a range of  $\pm 25^\circ$ .

## Results

**Thermal Denaturation.** To evaluate stability for structural studies, the thermodynamic parameters were measured for a size-extended (xDNA) duplex and a normal control duplex by van't Hoff analysis. Two similar self-complementary sequences, 5'-d(xATxAxATxATTxAT) and 5'-d(ATAATATTAT), were chosen for comparison (see Figure 1 for structures and numbering). Thermal denaturation behavior for these duplexes was studied by UV absorption at five different concentrations (2.0–12.0  $\mu$ M duplex) in a buffer containing 100 mM NaCl, 10 mM

(11) Koradi, R.; Billeter, M.; Wüthrich, K. *J. Mol. Graphics* **1996**, *14*, 51–55.

(9) Goddard, T. D.; Kneller, D. G. *SPARKY 3*; University of California: San Francisco, CA, 1995.

(10) Brüger, A. T.; Adams, P. D.; Clore, G. M.; Delano, W. L.; Gros, P.; Grosse-Kunstleve, R. W.; Jiang, J. S.; Kuszewski, J.; Nilges, M.; Pannu, N. S.; Read, R. J.; Rice, L. M.; Simonson, T.; Warren, G. L. *Acta Cryst.* **1998**, *D54*, 905–921.

**Table 1.** Thermodynamic Parameters for DNA and xDNA

sequence	$T_m$ (°C) at 5 $\mu$ M	$\Delta G_{310K}$ (kcal/mol)	$\Delta H$ (kcal/mol)	$\Delta S$ (cal/(mol·K))
xDNA	54.9 $\pm$ 0.5	-9.5 $\pm$ 0.2	-37.0 $\pm$ 3.6	-88.7 $\pm$ 10.9
DNA	20.1 $\pm$ 0.5	-3.7 $\pm$ 0.3	-68.1 $\pm$ 5.2	-207.8 $\pm$ 17.6

MgCl<sub>2</sub>, and 10 mM sodium PIPES buffer at pH 7.0. The xDNA duplex was monitored at 325 nm, where absorbance changes are greatest, while the natural duplex was monitored at 260 nm. The  $T_m$  values at 5.0  $\mu$ M duplex for extended DNA and control were 54.9 and 20.1 °C (Table 1), respectively. Free energies (37 °C) derived from van't Hoff plots for the extended DNA and normal DNA were -9.5 and -3.7 kcal/mol, respectively. Examination of enthalpy and entropy changes for the duplexes show (Table 1) that the largest difference arises in the entropy term, which is less unfavorable for xDNA than DNA helix formation. This suggests the possibility that the added stability of the xDNA helix might arise from prestacking of the single-stranded state; this is also consistent with the positive slope of the upper baseline of the melting curve. Overall, the results show that the extended duplex is much more stable than the normal duplex and would be expected to be stable under the conditions of structural studies (below). Additionally, the fact that melting temperatures change with varied duplex concentrations confirms formation of a duplex rather than a unimolecular hairpin.

**NMR Spectroscopy.** The symmetry of the self-complementary xDNA sequence results in five unique base pairs of duplex with 10 chemically distinct nucleotides. All nonexchangeable and thymidine imino proton resonances (for the 1D imino-proton spectrum see Figure S1 in SI) were assigned for the xDNA complex 5'-d(xATxAxATxATTxAT)<sub>2</sub> (Table S1) except for the terminal thymidine imino resonance, which was broad, presumably due to solvent exchange. The overall spectral quality was good; an example of the NMR data is shown in a <sup>13</sup>C/<sup>1</sup>H HSQC spectrum presented in Figure 2. In the HSQC experiment, the protons of the DNA duplex are observed in distinct chemical shift ranges of the 2D spectrum according to the chemical shift of the attached carbon atom. Optimally, there should be one distinct resonance for each proton/carbon pair as the protons disperse in chemical shift due to differences in local environment of a structured duplex. The dispersion of the xA C6/H6, xA C9/H9, and T C6/H6 are shown, with a nearly 1.3 ppm range of chemical shifts for the xA H6 protons, indicating quite different local environments for these five protons.

NOESY spectra acquired in D<sub>2</sub>O and H<sub>2</sub>O were used to determine <sup>1</sup>H/<sup>1</sup>H distance constraints for the duplex. Most standard internucleotide and intranucleotide NOEs observed in normal DNA were observed in this modified DNA duplex, including intranucleotide and sequential H1'-H2/6, H2'-H2/6, and H3'-H2/6 NOE signals. The additional protons on the modified benzo adenine base relative to adenine led to additional intranucleotide NOEs between the H4 and the H1', H2', and H3' protons. In addition, many nonstandard NOEs were observed between the protons on the aromatic bases in the base pairs above or below, including NOEs such as H6-H4, H9-H4, and H9-H9 from nucleotides on the opposite DNA strand. These base-stacking NOEs were helpful in structure determination.

**Structure of the Ten Base-Pair xA-T Duplex.** The structures of the 10 base-pair xDNA duplex were calculated from 394

NOEs and 90 experimentally determined dihedral constraints. Starting from two unfolded single strands with 30 randomized initial velocities, 24 structures converged to low energy. The structural statistics for the set of 24 converged structures are presented in Table 2. The superposition of these structures is presented in Figure 3. The overall heavy-atom rmsd for the 10 nucleotide duplex is 0.84 Å. The primary reasons for disorder of the duplex are slight changes of helical bending, which is difficult to define by NMR because of the lack of long-range constraints, and disorder at the terminal base pair, which is common as there are fewer internucleotide NOEs to terminal nuclei. When the terminal two base pairs were excluded from the superposition and the core residues of the duplex were superimposed (Figure 3b), the core residues have an rmsd of 0.53 Å.

**xDNA Resembles DNA.** The solution structural characterization by high-resolution NMR revealed that the structure of this xDNA (Figure 4) is similar to B-DNA in many aspects. Besides having righthandedness, this extended helix has identical Watson-Crick hydrogen bond patterns as those in B-DNA. In addition, all glycosidic bond conformations are anti and all deoxysugar conformations are 2'-endo, as are the cases for natural B-DNA. However, because of the size expansion of xA, the duplex diameter (as measured by P-P interstrand distance) is increased by ~3.0 Å (Table 3).<sup>12</sup> This larger diameter is reflected in widened groove dimensions (see below).

Another result of the extended diameter is that the xDNA helix has a greater number of base pairs per turn of the helix than natural DNA (which has ~10.5 pairs per turn). Except for being wider, our NOE-restrained model suggests that xDNA has two more base pairs per turn than B-DNA. This is primarily a result of reduced helix twist in xDNA, which is 31°, on average, as compared with 36° in B-DNA.

Another distinct feature of xDNA is that inter-base-pair distance is only 3.1 Å, about ~0.3 Å less than that in B-DNA. This shorter rise per base pair but greater base pairs per turn in xDNA results in a helix pitch of 37 Å. In comparison, B-DNA has a helix pitch of 34 Å, resulting from rise per base pair of 3.4 Å and 10 base pairs per turn. In contrast to straight helix of B-DNA, xDNA seems to have a slightly bent structure. However, given the limited ability of the currently used NMR methods to define longer-range structure, no definitive conclusion can be drawn for the overall shape of xDNA. We attempted to examine this independently by small-angle X-ray diffraction at the Stanford Synchrotron Research Laboratory, but data were inconclusive because of the short length and large diameter of this xDNA helix.

**Stacking Comparison.** In a similar manner as DNA, base pairs in xDNA stack on each other (Figure 5). The fact that helix twist varies in DNA (from 24° to 51°) is also true in xDNA. It seems that specific helix twist angles are consequences of stacking of neighboring xA bases. In case of consecutive xA's on the same strand, the twist angle is ~36°. However, when neighboring xA's reside on opposite strands, the twist angle is only ~22°. As shown in Figure 5 (top), neighboring xA's from opposite strands tend to show nearly maximal overlap of six-membered ring heterocycles. However, xA bases tend to

(12) Bloomfield, V. A.; Crothers, D. M.; Tinoco, I., Jr. *Nucleic Acids: Structures, Properties, and Functions*; University Science Books: Sausalito, CA, 1999; pp 90.



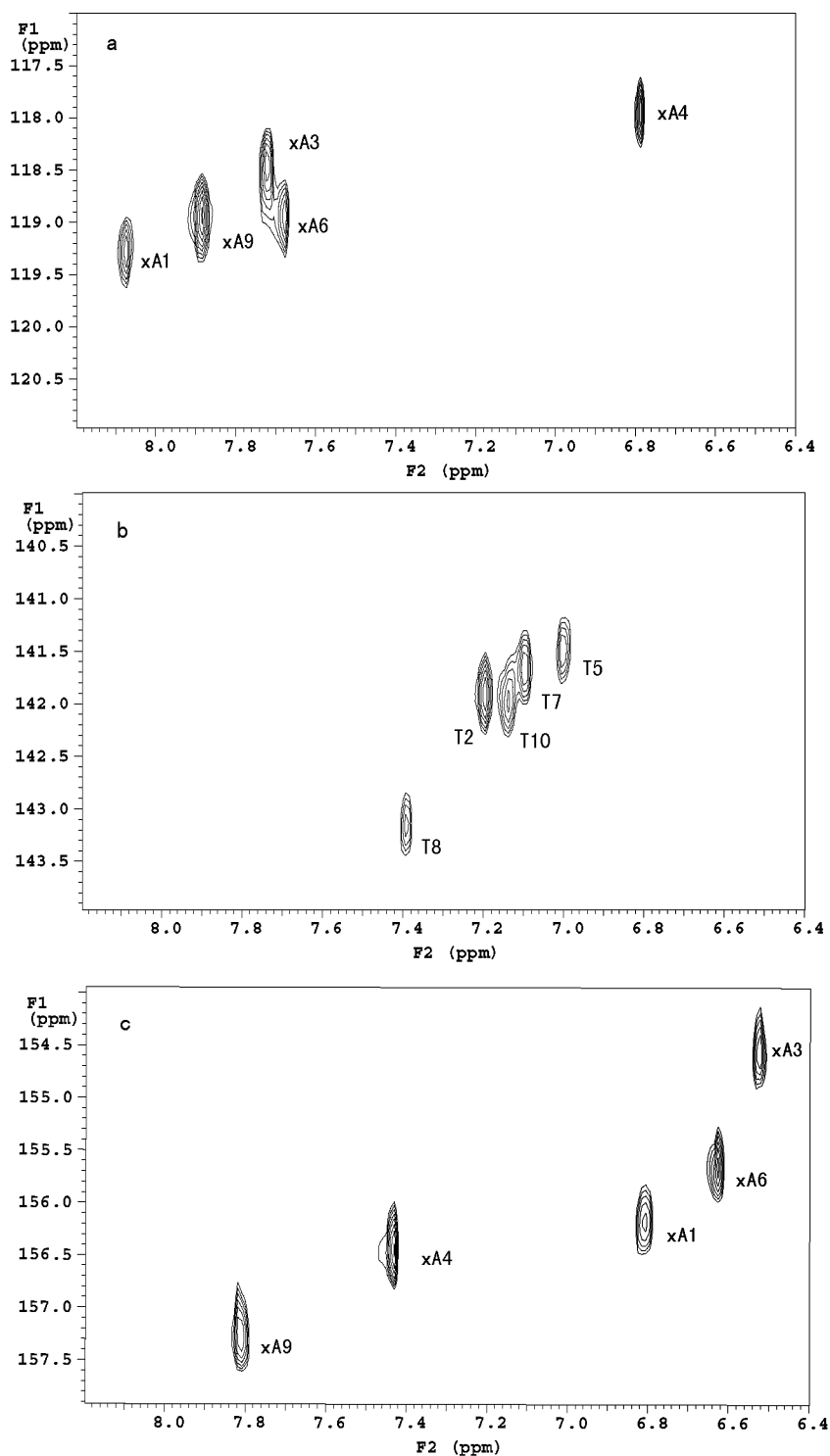


**Figure 2.**  $^{13}\text{C}/^1\text{H}$  HSQC spectrum of xA-T 10-nucleotide duplex acquired at 35 °C, showing three of the aromatic proton/carbon correlations. (a) The xA H9/C9. (b) The T H6/C6. (c) The xA H6/C6.

adopt a shifted stacking pattern when they are neighbors on the same strand (Figure 5, bottom).

**Comparison of Groove Structure.** The change in duplex diameter also results in changes in major and minor groove structures (Figure 6). Clearly, increased base-pair length pushes the backbones further apart. To accommodate an optimum stacking geometry, orientations of backbones are changed accordingly. As a net result of all these changes, base pairs are closer and grooves are wider. In comparison to the grooves of the A–T duplex control, the major groove of this xDNA duplex

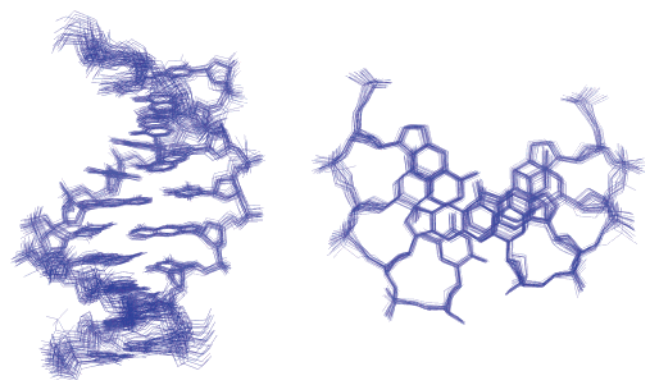
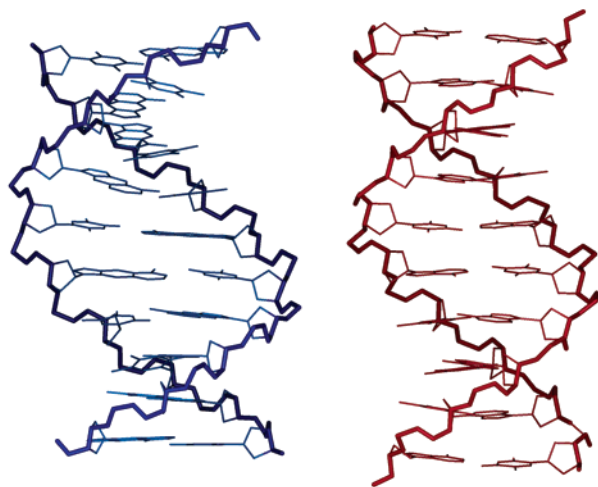
is 2.9 Å deeper and 2.5 Å wider, while the minor groove remains as deep and becomes 2.2 Å wider.

## Discussion

To survive in evolving systems, the molecules of life must exhibit advantages over alternative structures that might arise. One may therefore ask, why did DNA evolve to have the structure that it currently has? Are there alternative structures that also could be viable for storage and transfer of genetic information? In this and other recent studies<sup>6</sup> we have begun

**Table 2.** Structure Statistics and Atomic rms Deviations

Distance Constraints		
total		394
intranucleotide		166
internucleotide		228
interstrand		26
dihedral constraints		90
hydrogen bonds (WC base pairs)		40
Final Forcing Energies (kcal/mol)		
distance and dihedral constraints		$23.4 \pm 1.1$
rmsd from distance constraints (Å)		0.03
rmsd from dihedral constraints (deg)		1.21
Deviation from Idealized Geometry		
bond (Å)		0.0042
angles (deg)		0.81
impropers (deg)		0.29
Heavy Atom rmsd		
all		$0.84 \pm 0.22$
core residues (3–8, 13–18)		$0.53 \pm 0.22$

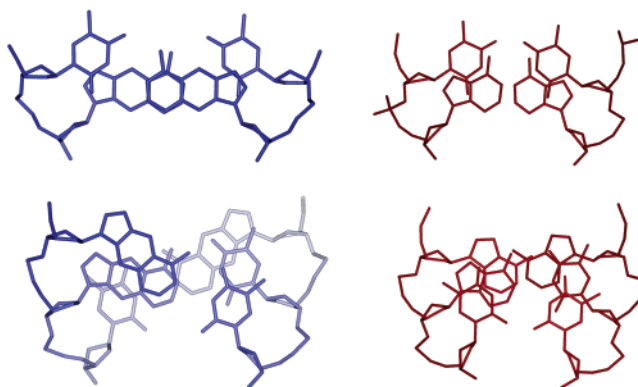
**Figure 3.** Superposition of 24 randomly selected final structures after restrained molecular dynamics and energy minimization.**Figure 4.** Mean structure of 24 randomly selected final structures of xDNA (at left) and a model structure of the control B-DNA (right).

to address these issues by asking whether the base pairs of DNA, the information-encoding part of the molecule, might be replaced altogether with new pairs of altered size. The current structural studies suggest that there is no apparent structural reason the base pairs could not be larger than those of natural DNA.

The fact that the phosphodiester backbone of the xDNA sequence studied here so closely resembles that of natural DNA was initially somewhat surprising. A simple analysis of xDNA structure suggests some possible reasons why the backbone

**Table 3.** Average Structural Parameters for xDNA and B-DNA (ref 13)

	xDNA	B-DNA
helix handedness	right	right
bp/repeating unit	1	1
bp/turn	12	10
helix twist (deg)	31	36
rise/bp (Å)	3.1	3.4
helix pitch (Å)	37	34
base-pair inclination (deg)	-0.5	2.4
diameter (Å)	21.4	18.4
X displacement from bp to helix axis (Å)	-2.0	-0.2
glycosidic bond orientation	anti	anti
sugar conformation	2'-endo	2'-endo
major groove depth width (Å)	7.0	4.1
	13.9	11.4
minor groove depth width (Å)	5.4	5.5
	8.1	5.9
Cl'-Cl' distance (Å)	13.3	10.7

**Figure 5.** Stacking of base pairs in the middle of xDNA (left) and in B-DNA (right). Top, xA or A residues on opposite strands; bottom, xA or A residues on the same strand.

might require some distortion. If one considers the helical backbone superimposed on the surface of a cylinder, increasing the diameter by ca. 2.4 Å is expected to increase the cylinder's circumference by 7.5 Å (ca. 20% greater than that of DNA). This suggests a conformational stretching of as much as 0.7 Å per nucleotide by rotating bonds, if twist per pair were that of normal DNA. Alternatively, if twist per step were lessened, this would result in an altered helix with as much as 14–16 pairs per turn. However, the actual finding is that the helix likely has only a more modest ~12 pairs per turn, which demonstrates the significant plasticity that small conformational rotations of backbone and glycosidic bond dihedrals lend to the helix.

The structural studies add insight into the surprisingly high thermodynamic stability measured for xDNA duplexes. Examination of the stacked structures of the bases show greater overlap in xA-T pairs with neighboring xA-T (or T-xA) pairs than occur in natural DNA. Preliminary studies using the dangling end methodology also suggest that xA stacks considerably more strongly than A does with neighboring base pairs.<sup>6a</sup> Another possible factor adding to the stability of xDNA might be reduced electrostatic repulsions from opposite strands that are further apart than those in natural DNA. However, preliminary studies have shown that this xDNA sequence has essentially identical ionic strength dependence as its DNA counterpart (H. Liu, J. Gao, E. T. Kool, unpublished data). Thus, combining all these observations, we conclude that exceptionally strong thermodynamic stability of xDNA is primarily a result of increased

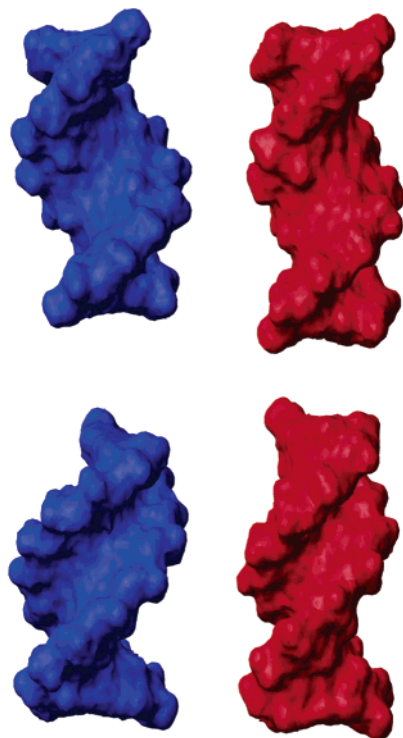


**Figure 6.** Space-filling models showing grooves of xDNA (blue, on left) and B-DNA (red, right). Top, major groove view; bottom, minor groove.

stacking due to larger aromatic surface of xA. Further thermodynamics studies, perhaps by calorimetry, would be useful for shedding more light on the sources of this stability. In addition, evaluating the effects of changing sequence on stability and structure will also be important in understanding the stability of xDNAs in general.

These early results allow us to reach some preliminary answers to questions posed in the Introduction. One of these was a basic question of molecular evolution: are there alternative base-pair structures that could be viable for storage and transfer of genetic information? Our results with xDNA have shown that extended pairs allow for selective and stable pairing in a double helical form, much like DNA. Thus we tentatively conclude that, at least for storage of genetic information, a molecular design like that of xDNA appears viable. It remains to be seen whether it would also be viable for transfer of information (i.e., synthesis of a complementary strand by polymerase enzymes). Of course, many of the biochemical

activities of DNA require local unwinding of the helix, and it is arguable that there may be evolutionary reasons to disfavor helices that are too thermodynamically stable. However, we note that some bacterial extreme thermophiles have evolved high G + C content in their genomes to add stability beyond that of average DNA sequences.<sup>14</sup> Use of larger base pairs might be an alternative to such a genetic strategy.

There is also the question of the energetic penalties for distortion of the DNA backbone away from that of a native conformation such as B-DNA. The present results suggest that quite significant changes to base-pair structure can readily be accommodated by the natural DNA backbone with little apparent penalty in overall stability. Importantly, the present case is that of a regular helix, in which every pair is extended in size and by an analogous amount and direction. Earlier preliminary studies have shown that single substitutions of extended pairs in an otherwise normal B-DNA base-pair context are, in fact, destabilizing to the helix.<sup>6a</sup> Similar findings of destabilization by local distortion have recently been reported by Minakawa et. al. with other multicyclic DNA base analogues as well.<sup>15</sup> Thus, regularity of the base-pair size is quite important to duplex stability. Further studies along these lines will be reported in due course.

Beyond the biological implications, the xDNA helix appears to be well-suited for molecular design applications. The stability and selectivity of the helix makes even short sequences quite stable at room temperature. The structural regularity and apparent rigidity of the xDNA helix are also promising in that respect. It does remain to be seen, however, whether the syntheses of the component nucleosides can be scaled up efficiently for widespread application.

**Acknowledgment.** We are grateful for support from the National Institutes of Health (GM63587). H.L. is the recipient of a Stanford Graduate Fellowship.

**Supporting Information Available:** 1D imino-proton spectrum, proton assignment table, and distance and torsion restraints (PDF). This material is available free of charge via the Internet at <http://pubs.acs.org>.

JA0497835

- (13) Stofer, E.; Lavery, R. *Biopolymers* **1994**, *34*, 337–346.  
 (14) Aleksandrushkina, N. I.; Egorova, L. A. *Mikrobiologiya* **1978**, *47*, 250–252.  
 (15) Minakawa, N.; Kojima, N.; Hikishima, S.; Sasaki, T.; Kiyosue, A.; Atsumi, N.; Ueno, Y.; Matsuda, A. *J. Am. Chem. Soc.* **2003**, *125*, 9970–9982.